SCIENTIFIC REPORTS
nature research

OPEN

Complementary roles of murine $Na_V1.7$, $Na_V1.8$ and $Na_V1.9$ in acute itch signalling

Helen Kühn[1*], Leonie Kappes[1], Katharina Wolf[1], Lisa Gebhardt[1,2], Markus F. Neurath[1], Peter Reeh[2], Michael J. M. Fischer[3,4] & Andreas E. Kremer[1,4*]

Acute pruritus occurs in various disorders. Despite severe repercussions on quality of life treatment options remain limited. Voltage-gated sodium channels (Na_V) are indispensable for transformation and propagation of sensory signals implicating them as drug targets. Here, $Na_V1.7$, 1.8 and 1.9 were compared for their contribution to itch by analysing Na_V-specific knockout mice. Acute pruritus was induced by a comprehensive panel of pruritogens (C48/80, endothelin, 5-HT, chloroquine, histamine, lysophosphatidic acid, trypsin, SLIGRL, β-alanine, BAM8-22), and scratching was assessed using a magnet-based recording technology. We report an unexpected stimulus-dependent diversity in Na_V channel-mediated itch signalling. $Na_V1.7^{-/-}$ showed substantial scratch reduction mainly towards strong pruritogens. $Na_V1.8^{-/-}$ impaired histamine and 5-HT-induced scratching while $Na_V1.9$ was involved in itch signalling towards 5-HT, C48/80 and SLIGRL. Furthermore, similar microfluorimetric calcium responses of sensory neurons and expression of itch-related TRP channels suggest no change in sensory transduction but in action potential transformation and conduction. The cumulative sum of scratching over all pruritogens confirmed a leading role of $Na_V1.7$ and indicated an overall contribution of $Na_V1.9$. Beside the proposed general role of $Na_V1.7$ and 1.9 in itch signalling, scrutiny of time courses suggested $Na_V1.8$ to sustain prolonged itching. Therefore, $Na_V1.7$ and 1.9 may represent targets in pruritus therapy.

Pruritus, commonly also referred to as itch, can appear as agonizing symptom of dermatological, systemic and psychogenic disorders[1]. Despite its high impact on the quality of life, treatment options remain limited. One obstacle in the development of new drugs arises from the diversity of signalling pathways triggering itch. Aside histamine, which was the first known pruritogen[2,3], pruritus can be elicited by various histamine-independent pruritogens with diverse chemical structures acting on a wide range of receptors. A major role in histamine-independent itch signalling can be attributed to Mas-related G protein-coupled receptors (MRGPR). This family of G protein-coupled receptors (GPCRs) mediates acute scratch behaviour towards pruritogens such as bovine adrenal medulla 8–22 peptide (BAM8-22)[4], chloroquine[5], β-alanine[6] and the tethered PAR2 ligand SLIGRL[7]. Additionally, pruritogens like 5-hydroxytryptamine (5-HT)[8], and lysophosphatidic acid (LPA)[9] signal via activation of their specific receptors.

Pruritogens can activate GPCRs located on nerve endings of unmyelinated primary sensory neurons, resulting in a rise of cytosolic calcium levels both via the inositol phospholipid signalling pathway[10–13] and via transient receptor potential ion channels (TRP)[14]. Upon membrane depolarization, voltage-gated sodium channels (Na_V) are opened, triggering the initiation and propagation of action potentials. The function of Na_V channels is determined by the pore-forming alpha-subunit of which nine subtypes with distinct functions have been identified[15]. Primary sensory neurons express virtually all subunits[16,17]. However, transcription analysis using single neuron RT-PCR and RNA sequencing have revealed a vast abundance of $Na_V1.7$, 1.8 and 1.9 in the slow conducting unmyelinated sensory neurons[18,19]. Complementary physiological studies have shown that these channels modulate pain signalling[20–22]. For their indispensable role in the generation and propagation of action potentials,

[1]Department of Medicine 1, Friedrich-Alexander-University Erlangen-Nürnberg, Ulmenweg 18, Erlangen, Germany. [2]Institute of Physiology and Pathophysiology, Friedrich-Alexander-University Erlangen-Nürnberg, Universitätsstrasse 17, Erlangen, Germany. [3]Center for Physiology and Pharmacology, Medical University of Vienna, Schwarzspanierstrasse 17, Vienna, Austria. [4]These authors contributed equally: Michael J. M. Fischer and Andreas E. Kremer. *email: helen.kuehn@fau.de; andreas.kremer@uk-erlangen.de

these Na_V subtypes have been suggested as potential drug targets for blunting sensory perceptions. Several subtype-specific Na_V inhibitors have lately entered clinical trials for different pain treatments[23–25].

Additionally, recent studies presented an important role of $Na_V1.7$–1.9 in itch signalling. Case studies revealed that gain-of-function mutations in these Na_V channels can cause paroxysmal itch in affected patients[26–29]. Corresponding inhibitory studies analysed the role of Na_V subtypes in itch signalling. Inhibition of $Na_V1.7$ reduced acute scratch behaviour in mice upon histamine and selected non-histaminergic stimuli[19,30–33]. Moreover, $Na_V1.9$ knockout mice showed reduced scratch behaviour upon treatment with histamine, chloroquine and BAM8-22[28]. This suggests that $Na_V1.7$ and $Na_V1.9$ are involved in acute itch signalling. While an isolated analysis of individual Na_V channels is sufficient to determine a role of Na_V subtypes in acute itch, the complexity of itch signalling with a possible complementing function of Na_V channels, as indicated by recent *in vitro* studies[18], remains elusive. To create a comprehensive picture of the role of Na_V channels in acute itch signalling we utilized knockout models for $Na_V1.7$, 1.8 and 1.9 and analysed the complementary roles of the Na_V channels for diverse itch stimuli. We show here that various pruritogens require different Na_V channels to mediate an itch stimulus while neuronal activation is unaltered in primary sensory neurons of the respective knockout animals.

Results

Acute itch stimuli signal via different Na_V channels. Scratch behaviour upon diverse acute itch stimuli was assessed in $Na_V1.7^{-/-}$, $Na_V1.8^{-/-}$, $Na_V1.9^{-/-}$ knockout mice and congenic wild type animals in order to explore which Na_V channels are required for itch signalling. All pruritogens were applied intradermally in the nape at concentrations which were, according to several publications, described to induce substantial itch (Fig. 1a–k). Scratch bouts were quantified for 30 min using an observer-independent, automated recording system. Scratching, assessed by a two-way ANOVA, showed a significant interaction of the between-subject factor 'genotype' and the within-subject factors 'pruritogen' ($F_{(30,430)} = 4.36$, $P < 0.0001$) but revealed no differences for the factor 'sex' ($F_{(1, 528)} = 1.48$, $p = 0.22$, including no interaction between 'sex' and 'genotype' $p = 0.55$, Supplementary Fig. S1 online). As the pruritogenic potential varied among the different pruritogens, we assessed the similarities in the induced scratch response in wild type mice using hierarchical cluster analysis with the Ward's method (Fig. 1m). The average scratch responses in wild type mice clustered into two groups. Thereby, the first cluster comprised pruritogens with strong and medium scratch responses (88–182 scratch events/30 min), namely C48/80, endothelin, 5-HT, chloroquine and histamine (Fig. 1b–f). The second group contained the pruritogens LPA, trypsin, SLIGRL, β-alanine and BAM8-22 inducing weaker scratching in mice (47–62 scratch events/30 min, Fig. 1g–k). All potent pruritogens from the first cluster showed a dependency on the expression of at least one of the investigated Na_V channels (Fig. 1b–f). $Na_V1.7$ knockout mice had a significantly reduced scratch behaviour upon C48/80 ($P = 0.001$), endothelin ($P = 0.002$), 5-HT ($P < 0.001$), chloroquine ($P = 0.028$) and histamine ($P < 0.001$, prespecified contrasts against wild type animals, Fig. 1b–f). $Na_V1.8^{-/-}$ exhibited a significantly reduced scratching upon 5-HT ($P = 0.009$) and histamine ($P = 0.006$), while $Na_V1.9$ knockout reduced the scratching upon C48/80 ($P = 0.017$) and 5-HT ($P < 0.001$).

Among the weaker pruritogens, SLIGRL-induced scratching was reduced upon $Na_V1.7$ and $Na_V1.9$ deletion ($P = 0.005$ and 0.033, prespecified contrasts against wild type animals). In contrast, the scratch responses upon the other weaker pruritogens were not significantly affected by the deletion of individual Na_V channels ($P = 0.166$–0.940, prespecified contrasts against wild type animals), albeit there was a trend towards reduced scratching activity in both $Na_V1.7^{-/-}$ and $Na_V1.9^{-/-}$ mice. Taken together, the grand sum of scratch responses over all pruritogens showed a 51.8% reduction of scratching in $Na_V1.7^{-/-}$ and 32.4% in $Na_V1.9^{-/-}$ but not in $Na_V1.8^{-/-}$ (post-hoc test for 'genotype'; $P < 0.001$, $P = 0.006$, $P = 1.0$, Fig. 1l) independent of the variance of individual pruritogens. Of note, all stimuli which were significantly modulated by $Na_V1.8$ or $Na_V1.9$ also exhibited a significant dependency on the expression of $Na_V1.7$.

Deletion of Na_V channels affects different phases of acute scratching. Time courses were scrutinized to assess which phases of scratching were affected by deletion of individual Na_V channels. Exploratory analysis of the time courses of scratching for the different stimuli showed different scratch patterns in the respective genotypes (Fig. 2a–l). The time-resolved grand sum of scratching exhibited in wild type mice an increase to a maximum at ten minutes after injection and then a linear decrease with a time constant of about 27 min (Fig. 2l). $Na_V1.7$ and $Na_V1.9$ knockouts showed the same pattern of time-related behaviour but on a much lower level of event counts (two-way ANOVA genotype x period $P < 0.0001$). In contrast, $Na_V1.8^{-/-}$ mice began at 5 min with the same high number of scratch events as wild types but then declined monotonously without a further peak. They clearly showed no scratch peak after injection of endothelin, 5-HT and histamine (Fig. 2c,d,f) resulting in reduced total scratching compared to wild type mice (Fig. 2m).

Pharmacological inhibition of $Na_V1.7$ and $Na_V1.8$ reduces acute scratching upon histamine and endothelin. To further corroborate the role of Na_V channels in acute itch signalling observed in genetic deletion models, we assessed the potential of $Na_V1.7$ inhibitor PF-05089771[34,35] and $Na_V1.8$ inhibitor A-803467[36] to alleviate acute scratching upon histamine and endothelin. As there is no specific $Na_V1.9$ inhibitor commercially available, the effects of pharmacological $Na_v1.9$ inhibition could not be assessed. Inhibition of $Na_V1.7$ by intraperitoneal pre-treatment of mice with PF-05089771 led to a reduced scratching upon histamine by 49.8% (paired t-test, $P < 0.001$) and upon endothelin by 45.6% (paired t-test, $P = 0.031$, Fig. 3a,b). Pharmacological inhibition of $Na_V1.8$ through intraperitoneal application of A-803467 prior to the intradermal pruritogen injection reduced scratch behaviour upon endothelin by 43.3% (paired t-test, $P = 0.003$) while the histamine response remained unaffected (paired t-test, $P = 0.77$, Fig. 3c,d).

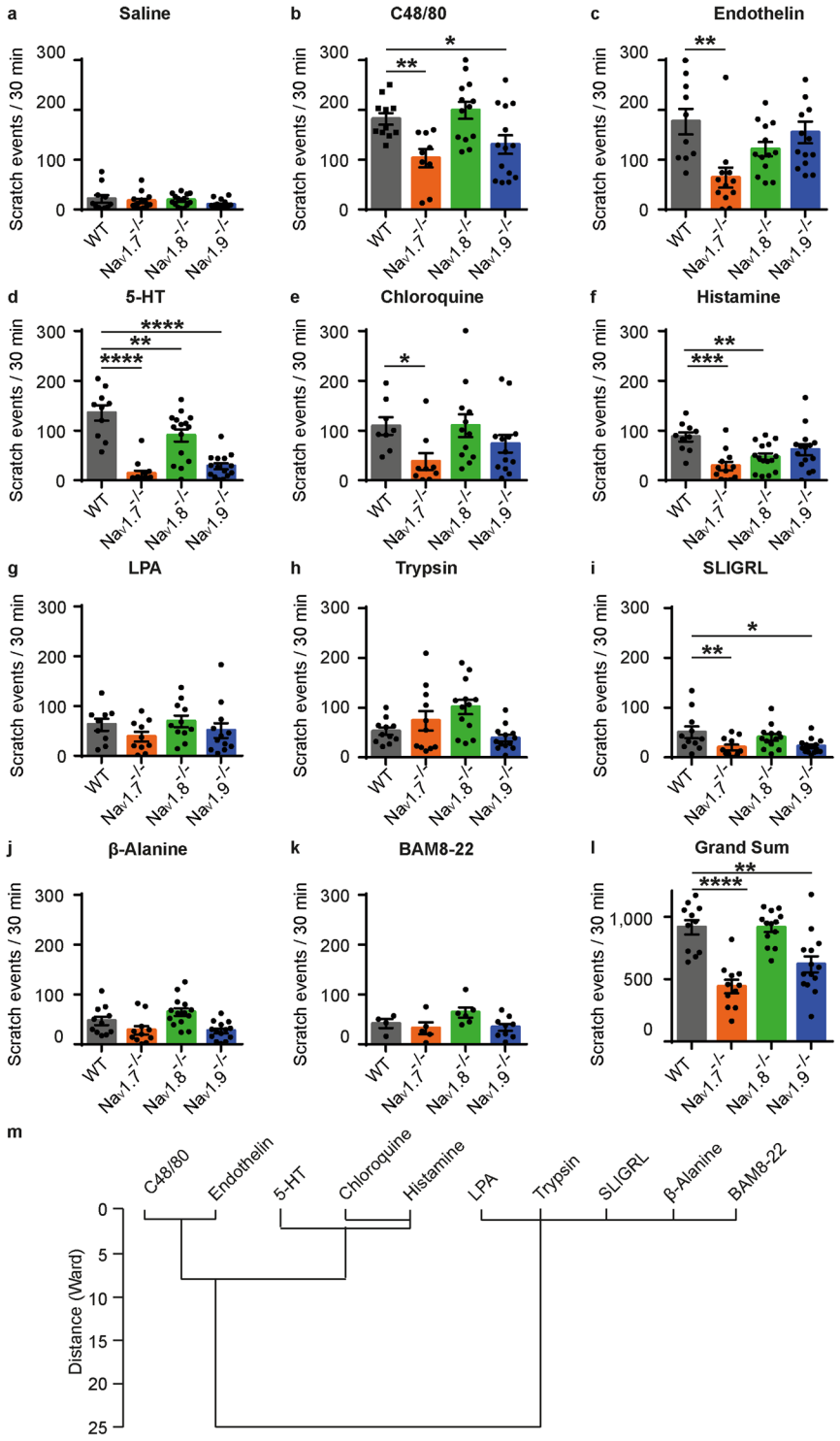

Figure 1. Acute scratch behaviour in $Na_V1.7^{-/-}$, $Na_V1.8^{-/-}$, $Na_V1.9^{-/-}$ and wild type mice upon intradermal injection of pruritogens. (**a–k**) Scratch events within 30 min after intradermal injection (50 µl) of saline, C48/80 (2 g/l), endothelin (1 µM), 5-HT (1 mM), chloroquine (4 mM), histamine (89 mM), LPA (4 mM), trypsin (10 U/µl), SLIGRL (2 mM), ß-alanine (224 mM) and BAM8-22 (1 mM). Pruritogens are displayed in order of potency, sorted according to the mean scratch behaviour induced in wild type mice. (**l**) Grand sum of the scratch behaviour across all pruritogens, n = 4–15, error bars: s.e.m, $^*P < 0.05$, $^{**}P < 0.01$, $^{***}P < 0.001$, $^{****}P < 0.0001$ (**m**) Hierarchical cluster analysis of the average scratch behaviour induced by each pruritogen in wild type mice using Ward's method.

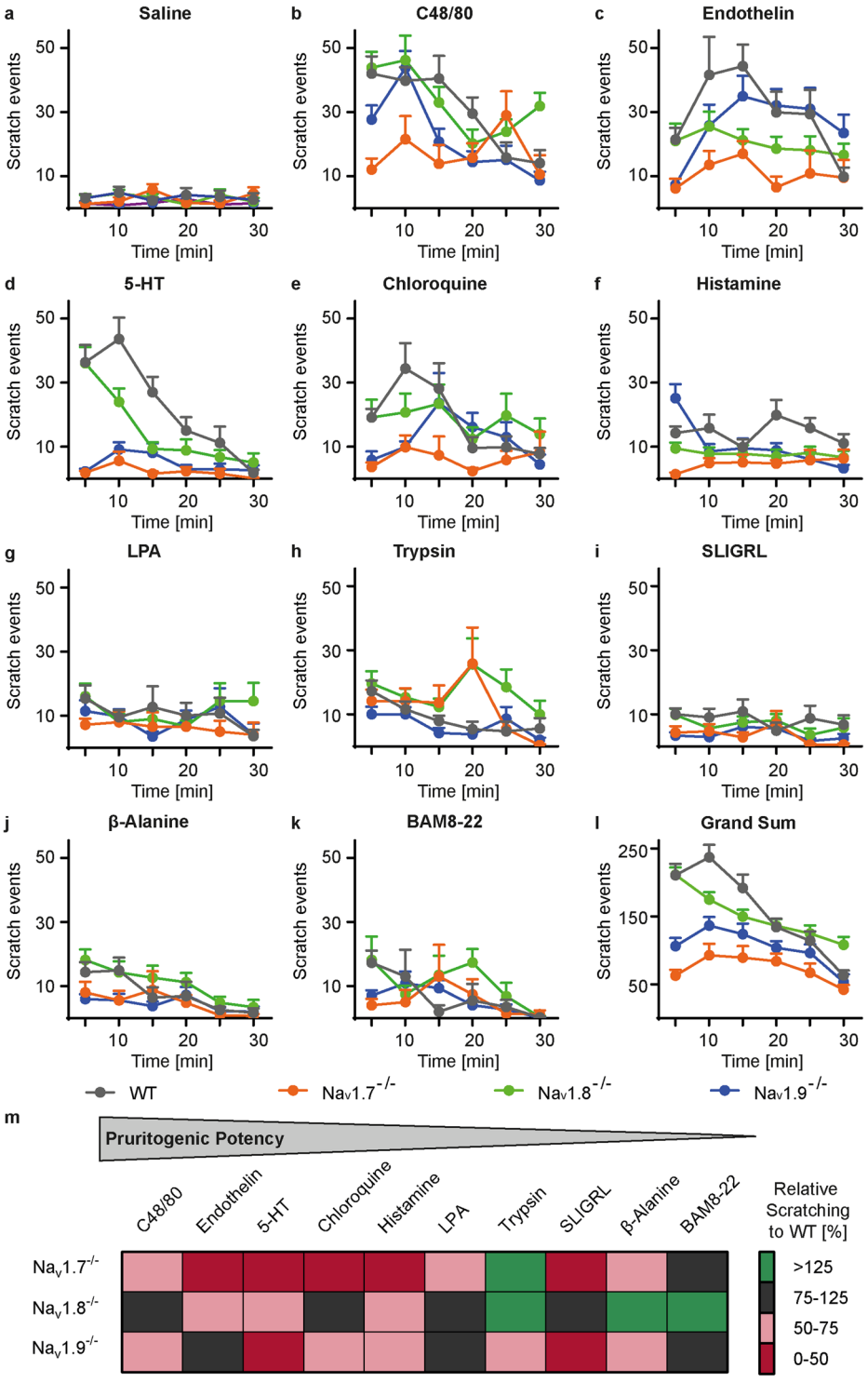

Figure 2. $Na_V1.7^{-/-}$, $Na_V1.8^{-/-}$ and $Na_V1.9^{-/-}$ mice exhibit different time-resolved scratch patterns. (**a–k**) Time course of scratch behaviour after intradermal injection (50 µl) of saline, C48/80 (2 g/l), endothelin (1 µM), 5-HT (1 mM), chloroquine (4 mM), histamine (89 mM), LPA (4 mM), trypsin (10 U/µl), SLIGRL (2 mM), ß-alanine (224 mM) and BAM8-22 (1 mM) (**l**) Grand sum of the scratch behaviour across all pruritogens; error bars: s.e.m (**m**) Heat map of the relative scratch behaviour in $Na_V1.7^{-/-}$, $Na_V1.8^{-/-}$, $Na_V1.9^{-/-}$ mice compared to wild type mice. Pruritogens are displayed in order of potency, sorted according to the mean scratch behaviour induced in wild type mice.

Activation of signalling pathways upstream of Na_V channels is equivalent in knockout and wild type mice. To verify that a reduction of acute scratch behaviour in knockout mice is related to a deletion of the respective Na_V channel and not caused by upstream effects, we compared the potential of the pruritogens

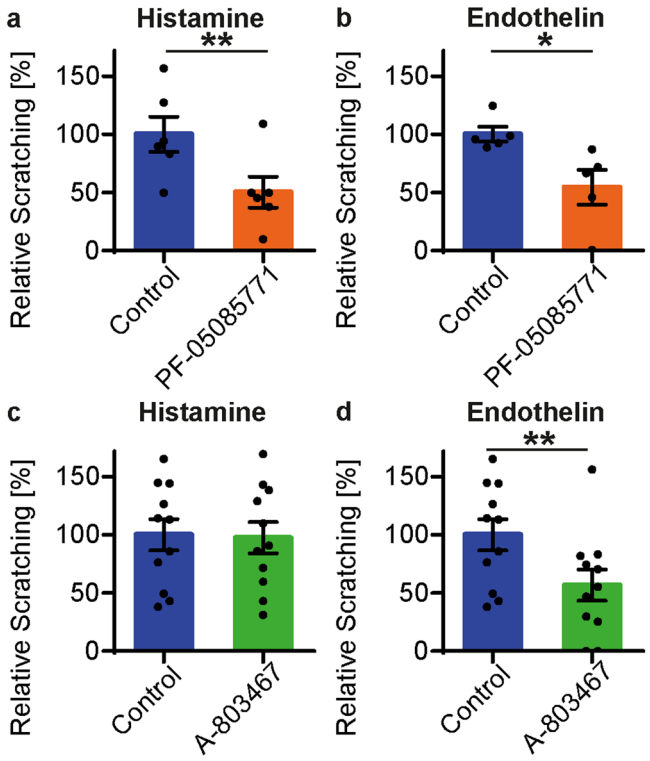

Figure 3. Reduction of histamine- and endothelin-induced scratching through $Na_V1.7$ and $Na_V1.8$ inhibition. Scratch behaviour upon intradermal injection of histamine (89 mM) and endothelin (1 µM) following inhibitor treatment relative to control response upon saline injection. (**a,b**) Pre-treatment with $Na_V1.7$ inhibitor PF-05089771 (i.p., 90 µg) 3 h prior to acute itch induction. (**c,d**) Pre-treatment with $Na_V1.8$ inhibitor A-803467 (i.p., 1.75 mg) 1.5 h before itch assessment. n = 5–12, error bars: s.e.m, $*P < 0.05$, $**P < 0.01$.

to activate dissociated dorsal root ganglia neurons (DRGs). Cultured sensory neurons of both wild type and knockout mice exhibited similar increases in cytosolic calcium upon addition of histamine, BAM8-22 and 5-HT (Fig. 4a–c). Furthermore, a similar percentage of neurons from wild type and knockout mice responded to histamine and serotonin, respectively (one-way ANOVA, $F_{(3, 11)} = 5.04$ & 0.33; $Na_V1.7^{-/-}$: P = 0.14 & 0.99; $Na_V1.8^{-/-}$: P = 0.33 & 0.97; $Na_V1.9^{-/-}$: P = 0.93 & 0.69). The corresponding pairwise scatterplots and respective Venn diagrams showed a similar distribution of neurons reacting to 5-HT and/or histamine in wild type and knockout animals (Fig. 4d–g). Accordingly, the histamine-induced transient cytosolic calcium increase displayed in the area under the curve was comparable in knockout and wild type animals (Fig. 4h–k).

Furthermore, we assessed the expression of the investigated Na_V channels on mRNA level. $Na_V1.7^{-/-}$ and $Na_V1.8^{-/-}$ revealed no compensatory up- or downregulation of the other Na_V channels on mRNA level, while $Na_V1.9^{-/-}$ mice showed a 4-fold upregulation of $Na_V1.8$ (U-Test, P = 0.036; Fig. 5a). As itch signalling pathways can be modulated by transient receptor potential ion channels (TRP), we further investigated the expression of TRPA1 and TRPV1 on mRNA and protein level. In agreement with the cellular responses detected by measurement of cytosolic free calcium levels, expression of TRPA1 and TRPV1 was comparable in knockout and wild type animals (Kruskal-Wallis Test, Fig. 5b–d). Corresponding immunofluorescence showed no difference in expression or localization of TRPA1 and TPRV1 in knockout- and wild type animals (Fig. 5c,d).

Discussion

Pruritus represents a clinical burden which can occur in various systemic diseases, under dermatological conditions and as adverse effect of countless therapies[1,37]. To date treatment options remain limited and the diversity of pruriceptors and signalling pathways involved as well as their redundancy represent major challenges in the development of novel anti-pruritic treatment strategies. As Na_V channels are comparably few but indispensable for the transformation and propagation of sensory signals, they represent common key players for the signalling of pruritus independent of its origin and have therefore been suggested as drug targets. To widen our knowledge about the role of Na_V channels in acute itch signalling, we compared the involvement of $Na_V1.7$, $Na_V1.8$ and $Na_V1.9$, performing behavioural studies with a comprehensive set of pruritogens in the respective knockout mice. The results revealed an unexpected diversity of the Na_V-mediated itch signalling depending on the acute stimulus applied. Deletion of either $Na_V1.7$, $Na_V1.8$ or $Na_V1.9$ had an impact on acute itch signalling albeit to different extents. $Na_V1.7$ deletion blunted most acute itch stimuli and $Na_V1.9$ had a robust overall effect on itch signalling, while $Na_V1.8$ deletion reduced scratch behaviour only towards certain strong stimuli and resulted in a different time course of scratching. Thereby, equal microfluorimetric calcium responses of sensory neurons in the regarded

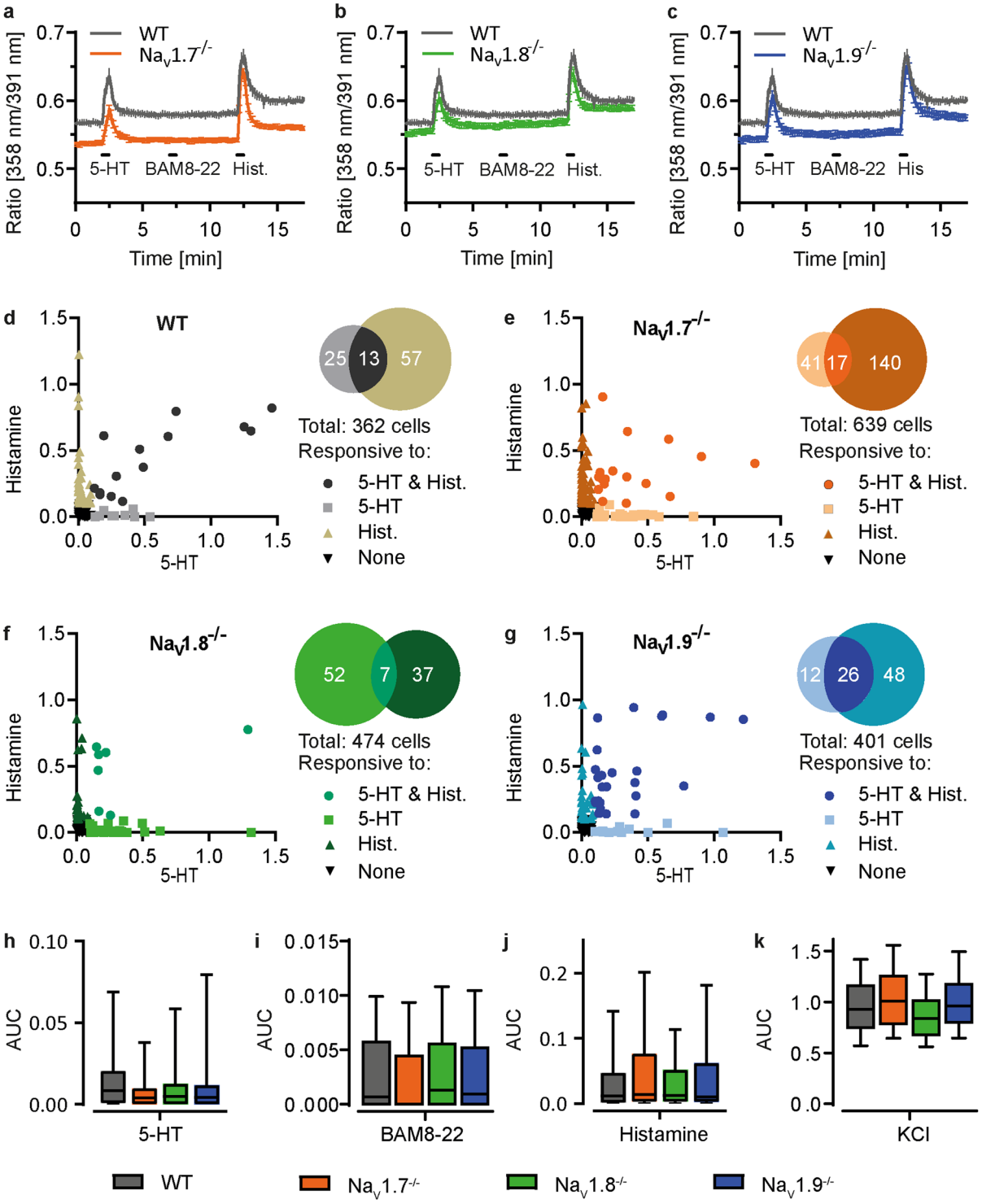

Figure 4. Dorsal root ganglion neurons from Na$_V$1.7$^{-/-}$, Na$_V$1.8$^{-/-}$, Na$_V$1.9$^{-/-}$ and wild type mice show similar calcium responses upon stimulation with 5-HT, BAM8-22 and histamine. (**a**–**c**) Average cytosolic calcium transients in dissociated, 1-day cultured dorsal root ganglion neurons upon stimulation with 5-HT (1.5 µM), BAM8-22 (2 µM), histamine (150 µM) and KCl (60 nM) as positive control. Bars indicate application periods. (**d**–**g**) Scatterplots of the ratio increases of individual neurons of Na$_V$1.7$^{-/-}$, Na$_V$1.8$^{-/-}$, Na$_V$1.9$^{-/-}$ and wild type mice responding to histamine and 5-HT. Venn diagrams illustrate the overlap between cells positive for either or both stimuli (**h**–**k**) Box plots of the corresponding area under the curve (AUC) for the first minute of application. Boxes display median and 25–75 percentiles; whiskers represent 10 and 90 percentiles.

genotypes and a similar expression of itch-related TRP channels, suggested no change in sensory transduction but in action potential transformation and conduction. Differences in scratch behaviour can therefore be attributed to Na$_V$ deletion and not to changes upstream of Na$_V$.

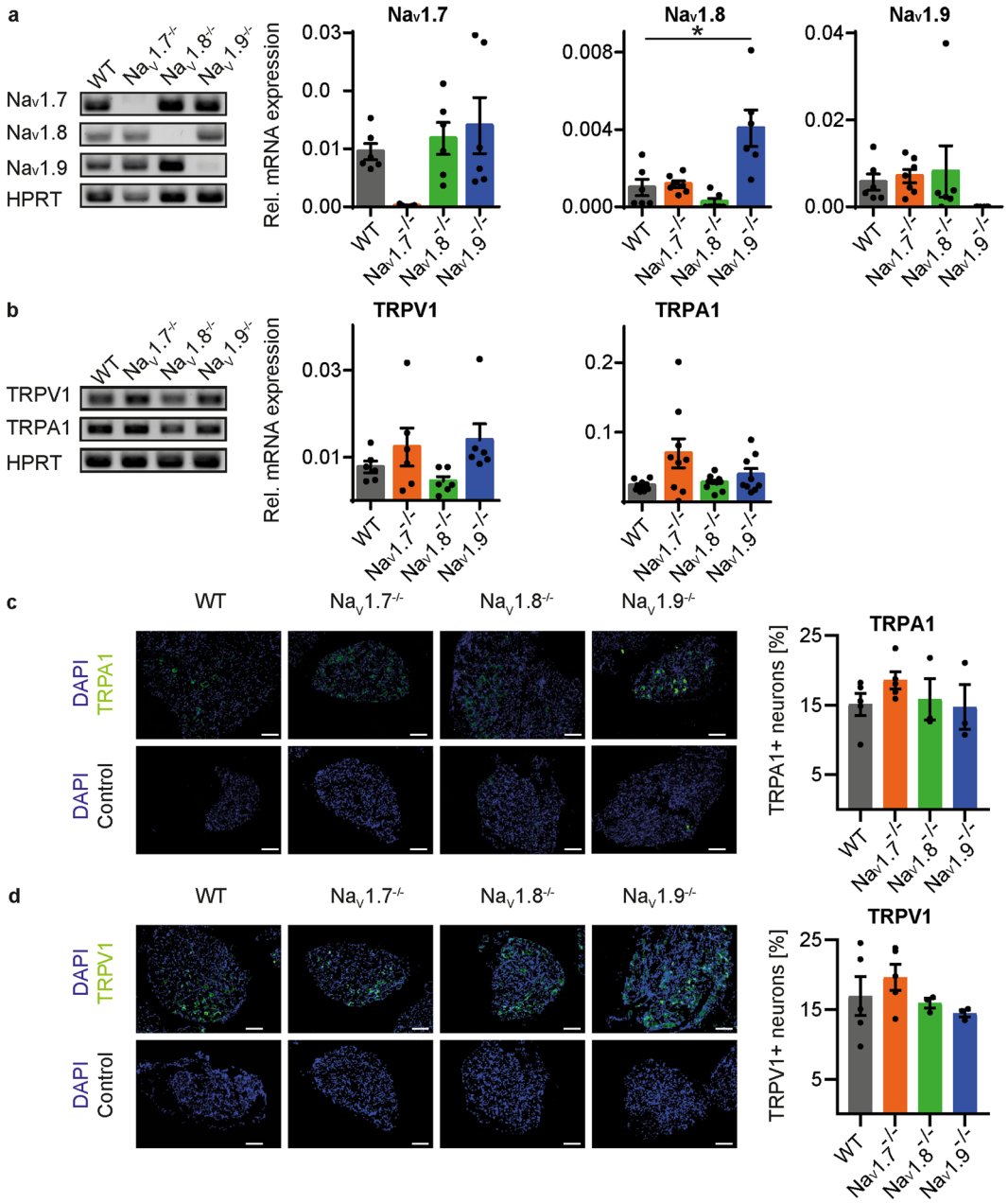

Figure 5. Expression of Na_V and TRP channels in dorsal root ganglion neurons of $Na_V1.7^{-/-}$, $Na_V1.8^{-/-}$, $Na_V1.9^{-/-}$ and wild type mice. (**a**,**b**) Relative mRNA expression compared to HPRT and respective agarose gels of amplified PCR products for Na_V, TRPA1 and TRPV1 channels. error bars: s.e.m, $*P < 0.05$ (**c**,**d**) Representative and quantitative immunohistochemistry of TRPA1 and TRPV1 expression, n = 3–5 (average from 4–7 slices per animal), error bars: s.e.m, scale bar: 100 µM.

Deletion of $Na_V1.7$ affected the signalling of all tested pruritogens – ranging from moderate to strong reduction of scratch behaviour. This goes in line with previous studies showing a reduction of histamine-, chloroquine- and C48/80-induced itch[30,31,38]. While those studies confirmed the role of $Na_V1.7$ for individual pruritogens, our results strongly suggest $Na_V1.7$ to be a key mediator of acute itch signalling independent of the stimulus applied. $Na_V1.7$ is characterized by a low threshold and rapid activation[39]. It has therefore been suggested to trigger action potentials and contribute to determining nociceptor excitability[40]. This hypothesis has been supported by observations in patients with inherited erythromelalgia caused by different point mutations in SCN9A. Mutations in the gene for $Na_V1.7$ lead to a hyperpolarizing shift of the voltage-dependent activation of the channel[41–43]. In contrast, loss-of-function mutations in the same gene lead to the Congenital Indifference to Pain (CIP) syndrome which includes the lack of pruritus[44]. The substantial reduction of scratching in $Na_V1.7^{-/-}$ and the failure of knockout mice to reach scratch peaks in comparison to the congenic wild type mice, indicate that this channel is most relevant for the transformation of itch stimuli in mice, though not indispensable. Of note, the used $Na_V1.7^{-/-}$ mouse strain underlies an Advillin-Cre based conditional deletion of $Na_V1.7$ in sensory neurons.

Therefore, a marginal neuronal $Na_V1.7$ expression cannot be ruled out and a germline knockout out model may show an even more prominent role of $Na_V1.7$ in acute itch signalling as suggested by Gingras *et al.*[45]. However, as $Na_V1.7$ mRNA expression in DRGs was undetectable, the risk of underestimating the $Na_V1.7$ expression and its influence on itch behaviour appears minimal.

Despite the high expression of $Na_V1.8$ in sensory neurons activated by itch and pain[18] as well as the occurrence of chronic pruritus in patients with a gain-of-function mutation[27], the role of $Na_V1.8$ in itch signalling remains poorly understood. Here, we show that $Na_V1.8$ modulates scratch behaviour induced, in particular, by the strong pruritogens 5-HT and histamine. Albeit there was not a uniform change in the responses to different pruritogens in $Na_V1.8^{-/-}$, the grand sum of scratch events across all applied pruritogens (Fig. 2l) suggests that the behavioural activity declines from an initial maximum without the normal exaggeration around 10 min after injection. This may be due to the particular $Na_V1.8$ capacity of "fast re-priming", i. e. fast recovery from voltage-dependent inactivation (brief refractory period). This allows high-frequency repetitive firing of action potentials[46–48] and thus continuation of high scratch levels. Knockout animals may lose this capacity which may shorten the scratching periods upon strong itch stimuli. Both deletion of $Na_V1.8$ and its pharmacological inhibition reduced endothelin-induced scratch behaviour in mice. Knockout animals showed an average reduction of 31% compared to wild type mice which is in line with 46% decrease during pharmacological inhibition. Although reduction of scratching in $Na_V1.8^{-/-}$ failed to reach significance ($P = 0.063$), effects of pharmacological inhibition strongly suggest biological relevance and involvement of $Na_V1.8$ in endothelin-induced scratching. Surprisingly, deletion of $Na_V1.8$ resulted in a significantly reduced scratching induced by histamine while pharmacological inhibition of $Na_V1.8$ failed to decrease scratch activity. Jurcakova *et al*. have recently shown that $Na_V1.8$ inhibition alone does not affect firing response of murine C-fibers upon chloroquine treatment, and dual inhibition of $Na_V1.7$ and 1.8 is needed to abolish this firing[18]. The sufficiency of sole $Na_V1.8$ inhibition to reduce acute itch signalling upon endothelin but not histamine, may indicate a different weight of Na_V channel participation during acute itch signalling depending on the distinct stimulus. This may finally lead to differential effects of single Na_V inhibitors.

The results further demonstrate that $Na_V1.9$ deletion results in a substantial overall reduction of acute scratching in the sum of all applied pruritogens and in particular upon intradermal injection of C48/80, 5-HT and SLIGRL. As in $Na_V1.7^{-/-}$, the reduction of scratch responses was most prominent during the first 15 min of observation. Recent studies showed that $Na_V1.9$ knockout mice exhibit a significantly elevated threshold to mechanical and heat stimuli and a reduced (electrical) excitability of skin nociceptors[49]. Taken together with our behavioural data, we suggest that $Na_V1.9$ modulates the transformation of acute itch stimuli, lowering the threshold to action potential generation. The effects observed in $Na_V1.9^{-/-}$ are less prominent than observations recently made by Salvatierra *et al*., who showed a reduction of scratch behaviour in $Na_V1.9$ knockout mice upon histamine, chloroquine and BAM8-22 when applying the substances subcutaneously[28]. While the nerve endings of primary sensory neurons largely terminate in the epidermis, other cellular players of itch signalling such as mast cells are distributed in the corium[50] which potentially modulate neuronal activation when applying pruritogens subcutaneously compared to an intradermal application.

Utilization of knockout models enables the directed examination of channel characteristics and investigates a link between behavioural phenotypes and the expression of the regarded molecule of interest. However, due to the general nature of knockout models, it cannot be excluded that further molecules up- and downstream of the respective Na_V channels are affected by the genetic modification and may influence the itch behaviour investigated here. Furthermore, knockout of $Na_V1.8$ has been shown to induce upregulation of $Na_V1.7$[20,51,52] while no indications of compensatory effects in $Na_V1.7^{-/-}$ and $Na_V1.9^{-/-}$ have been reported[53,54]. Although, compensation could affect behavioural phenotypes of the knockout mice, an upregulation of $Na_V1.7$ in $Na_V1.8^{-/-}$ cannot explain the phenotype observed here. $Na_V1.8^{-/-}$, lacking the fast re-priming sodium channel, exhibit a normal onset of scratching compared to wild type mice but fail to reach scratch peaks as detected in the grand sum over all pruritogens. In contrast, the tetrodotoxin-sensitive $Na_V1.7$ has a slow recovery from fast voltage-dependent inactivation[55,56] and can therefore not trigger high frequency spiking which occurs with strong pruritogens after injection. Consequently, the observed behavioural abnormalities of $Na_V1.8^{-/-}$ can be attributed to the deletion of $Na_V1.8$ and are not a result of $Na_V1.7$ upregulation.

In agreement with previous studies, we show that a deletion or inhibition of one Na_V channel is not sufficient to fully abolish scratching in mice[28,30–33]. The contribution of several Na_V channels to acute itch signalling of different stimuli, shown here, supports the suggestion that a simultaneous inhibition of different Na_V channels is required to reach full abolishment. This is in line with recent studies on *ex vivo* DRG-nerve-skin preparations reporting that tetrodotoxin suppressed firing in 75% of the fibers, $Na_V1.7$ selective blockage in 40% of itch C-fibers, but the combination of $Na_V1.7$ and $Na_V1.8$ inhibition resulted in full abolishment of action potential discharge[18]. Contrary, in human case studies a loss-of-function mutation of $Na_V1.7$ resulted in absence of itch perception[44]. As $Na_V1.7$ deletion has been shown to cause an increased efficiency of antinociception via μ-opioid receptors[57], which are involved in itch signalling[58], it may be possible that μ-opioid signalling effects itch sensitivity in the knockout mice. Furthermore, thin myelinated A-fibers, which express $Na_V1.6$ as action potential generator in their nodes of Ranvier, have been shown to contribute to cowage- and histamine-induced itch in primates and humans[59] and could maintain acute itch signalling to some extent.

In summary, our results demonstrate an involvement of $Na_V1.7$, 1.8 and 1.9 in acute signalling. Scrutiny of the scratch pattern in knockout mice revealed a role of Na_V in different phases of acute scratching. According to our behavioural data, $Na_V1.7$ and 1.9 generally participate in itch signalling, while $Na_V1.8$ sustains prolonged itching. Unravelling these molecular mechanisms of itch signalling in the primary sensory neurons will have a major impact on the development of new therapies. In case of acute pruritus, we suggest that $Na_V1.7$ and 1.9 may provide targets in pruritus therapy.

Methods

Animals. $Na_V1.7^{-/-}$ mice exhibited an Advillin promoter-dependent deletion of exon 14 and 15 of the SCN9A gene, preventing functional expression of $Na_V1.7$ in dorsal root ganglia (DRG) and trigeminal ganglia neurons[60]. $Na_V1.8^{-/-}$ and $Na_V1.9^{-/-}$ were generated by deletion of exon 4–5 of SCN10A and SCN11A, respectively, as described before[51,54]. Knockout was confirmed by genotyping as described earlier[51,54,60]. Animals from both sexes with an age from 11 to 19 weeks, bred in house, were used for experiments. Mice were housed in a regulated 12 h day-night cycle with water and nutrition ad libitum. As the knockout strains are backcrossed to C57BL/6 J every 3–4 generations, congenic; age- and sex-matched C57BL/6 J mice were used as controls. Animals were killed in a rising CO_2 atmosphere and by cervical dislocation. The present study was performed in accordance institutional, national and international guidelines and regulations. All experiments were approved by the institutional animal care (Sachgebiet Tierschutz, Friedrich-Alexander University, Erlangen, Germany) and the district government (55.2.2-2532-2-642-11; Regierung Unterfranken, Würzburg, Germany).

Behavioural itch assay. The behavioural testing to asses scratch behaviour was conducted as described previously[9]. Briefly, small Teflon-coated magnets were implanted into both hind paws of the experimental animals one week prior to behavioural experiments. The mice were given 60 min to acclimatize to the individual measurement cages before intradermal injection of 50 µl saline or the respective pruritogens into the nape using a 30 G fine dosage syringe (Braun, Kronberg im Taunus, Germany). The mice were injected on 6 consecutive days. After injection of saline on day 1 5-HT (1 mM, Biomol, Hamburg, Germany), histamine (89 mM, Carl Roth, Karlsruhe, Germany), endothelin (1 µM, Enzo, Farmingdale, NY, USA), chloroquine (4 mM, Sigma Aldrich) and LPA 18:1 (4 mM, Avanti Lipids, Alabaster, AL, USA) were applied. After 3 days of rest, consecutive injections of β-alanine (224 mM, Sigma Aldrich, St. Louis), C48/80 (2 g/l, Sigma Aldrich, St. Louis, MO, USA), SLIGRL (2 mM, Biomatik, Cambridge, ON, Canada), trypsin (10 U/µl, Sigma Aldrich) and BAM8-22 (1 mM, Genemed Synthesis Inc., San Antonio, TX, USA) were performed. Power analysis was conducted beforehand to estimate the required animal numbers using G*Power software (Version 3.1.9.2)[61]. All genotypes underwent the same application procedures. A substance-independent sensitization of the animals due to consecutive injections was excluded by unchanged scratch responses upon saline injection before and after other itch-inducing stimuli. Furthermore, application order was potency adapted varying between strong and weak pruritogens. The repeated administration did not cause any visible local damage to the skin, which was checked each day before intradermal administration of the substances. The protocol and experimental design was known to the experimenter since the automated scratch recording guaranteed unbiased scratch assessment. Immediately after injection, scratch behaviour was assessed for 30 min. Scratches were automatically detected as the movement of the implanted magnets induced electric currents in two coils around the cages, recorded using oscillography. Recordings were controlled by SiMon (V2.0, Academic Medical Center, University of Amsterdam, the Netherlands) and analysed offline by Scratch Analysis (V1.13, Academic Medical Center, University of Amsterdam, the Netherlands). Movements were classified as scratching based on their frequency (10–20 Hz), the amplitude of the signals (above 300 mV) and a minimum of 4 repetitions. For this methodical approach a positive prediction value of 95% was shown before[9].

For pharmacological inhibition of $Na_V1.7$, 90 µg of PF-05089771 (Sigma Aldrich) were dissolved in extracellular solution (145 mM NaCl, 4.96 mM KCl, 1.62 mM $CaCl_2$, 0.98 mM $MgCl_2$, 10 mM Glucose, 10 mM Hepes, pH: 7.4) supplemented with 1% dimethyl sulfoxide (DMSO, Carl Roth) and applied intraperitoneally 3 h prior acute itch measurement. $Na_V1.8$ was inhibited using 1.75 mg of A-803467, dissolved in polyethylene glycol 400 (PEG 400, Sigma Aldrich) supplemented with 5% DMSO and applied intraperitoneally 1.5 h before scratch measurement. The control groups underwent the same experimental procedures but received intraperitoneal injection of the respective solvent.

Immunofluorescence. For DRG isolation, the spinal column of sacrificed mice was removed and incubated for 2 h in 4% paraformaldehyde (PFA). Subsequently, DRGs were isolated and incubated for another 30 min in 4% PFA before being transferred to phosphate buffered saline (PBS) followed by 20% sucrose solution each for 24 h at 4 °C. Then, the tissue was embedded in Tissue-Tek O.C.T. Compound (Sakura Alphen aan den Rijn, The Netherlands), sliced to 14 µM sections using a Leica CM3050S cryostat (Leica, Wetzlar, Germany) and embedded on microscope slides coated with Poly-L-Lysine. After thawing the microscope slides for 1 h at room temperature (RT) and washing the tissue in PBS, unspecific binding sites were blocked in PBS supplemented with 0.5% Triton X-100 (Sigma Aldrich), 1% bovine serum albumin (Sigma Aldrich) and 5% donkey serum (Dianova, Hamburg, Germany) for 1 h at RT. After washing the tissue with PBS, the primary antibody for TRPV1 (Neuromics, Edina, MN, USA; RA14113, polyclonal rabbit, 1:1000) or TRPA1 (abcam, Cambridge, UK; ab62053, polyclonal rabbit, 1:1000) was diluted in blocking solution and incubated overnight at 4 °C. Subsequently, the tissue sections were washed in PBS before incubating the appropriate secondary antibody (donkey-anti-rabbit-Alexa 555, Molecular Probe, Eugene, OR, USA, A-31572, 1:1000) for 1 h at RT. After repeated washing with PBS, the tissue sections were mounted with Roti-Mount FluorCare DAPI (Carl Roth, Karlsruhe, Germany) and staining was visualized using a Leica DM 6000B upright and a Leica TCS SP8 confocal microscope operated by Leica application suite. Images were acquired with a 0.5 NA 20x objective lens and the confocal pinhole was set to 1 Airy unit. The Alexa555-labeled secondary antibody was detected with the 488 nm laser line at emission wavelengths from 493 nm–739 nm. DAPI was measured with the 405 nm laser line at emission wavelengths from 410 nm–493 nm.

Fluorometric measurement of cytosolic free calcium levels. Isolated DRGs from $Na_V1.7^{-/-}$, $Na_V1.8^{-/-}$, $Na_V1.9^{-/-}$ as well as wild type mice were digested in extracellular solution supplemented with 0.5% streptomyces proteinase and 1% clostridium collagenase (Sigma Aldrich, St. Louis, MO, USA) at 37 °C and 5% CO_2 for 30 min. Thereafter, the dissociated cells were plated on cover slides precoated with Poly-D-Lysine, and cultivated for 14–20 h in TNB100 Medium supplemented with TNB 100 protein-lipid complex (Biochrom,

Berlin, Germany), penicillin and streptomycin (100 U/ml each, Life Technologies, Carlsbad, CA, USA) and nerve growth factor (mouse NGF 2.5 S, 100 ng/ml; Alomone Labs, Tel Aviv, Israel). For calcium imaging, the cells were loaded with the calcium sensitive dye Fura2-AM (3 µM, Biotium, Fremont, CA, USA) diluted in extracellular solution supplemented with 0.02% pluronic F-127 (ThermoFisher Scientific, Waltham, MA or Biotrend, Cologne, Germany). Loading was performed for 30 min at 37 °C and 5% CO_2. After washing, cover slides were placed on an inverted microscope and samples were excited at 358 und 391 nm with a Polychrome V monochromator (Till Photonics, Graefelfing, Germany) at 1 Hz. A gravity driven and software-controlled common outlet perfusion system[62] allowed the continuous superfusion of the cells at a rate of 0.5 ml/min. A peltier-cooled slow-scan CCD camera collected the fluorescence emission above 440 nm. Using this perfusion system cells were treated with 1.5 µM 5-HT, 2 µM BAM8-22, 150 µM histamine for 30 s and 60 mM potassium chloride (KCl) for 20 s. All substances were dissolved in extracellular solution. TillVision software (ThermoFisher Scientific) was used to control the experiments, to analyse the data and to calculate the fluorescence ratio (358/391 nm) for all regions of interest after background subtraction. Cells with an increase of fluorescence intensity of minimum 0.1 were considered responding. Negative ratios were set to 0. The area under the curve (AUC) of the ratio within one minute after start of application was calculated. All protocols contained a final application of KCl to discard non-vital and non-neuronal cells.

Quantitative real-time PCR. Immediately upon isolation, DRGs were transferred to TRIzol (Thermo Fisher Scientific) and homogenized using a TissueLyser (Qiagen, Hilden, Germany). Subsequently, RNA was isolated according to manufacturer's protocol (TriZOL, Thermo Fisher Scientific). The quality of RNA was assessed using a Nanodrop ND1000 Spectrophotometer (Thermo Fisher Scientific). Complementary DNA was synthesized from 500 ng to 1 µg RNA using oligo-dT primer and SCRIPT cDNA Synthesis Kit (Jena Bioscience, Jena, Germany). Quantitative real-time PCR was performed for 40 cycles at an annealing temperature of 60 °C using SensiFast Sybr No-ROX Kit (Bioline, London, UK) in a CFX Connect qPCR System (Bio-Rad Laboratories, Hercules, CA, USA). Primer sequences are listed in supplementary table S1. The detected quantification cycles (C_q) were normalized to C_q values of the housekeeping gene hypoxanthin-guanin-phosphoribosyltransferase (HPRT) using the $2^{-\Delta\Delta CT}$ method[63]. The amplified DNA products were separated by agarose gel electrophoresis on a 2% agarose gel supplemented with Midori Green Advanced (Nippon Genetics Europe, Dueren, Germany) and visualized using a Gel Doc XR + Gel Documentation System (Biorad, Hercules, CA, USA).

Data analysis. Statistical analyses were carried out using Sigmaplot (Version 12.5, Systat Software Inc., Erkrath, Germany) and GraphPad Prism Version 7 and 8 (GraphPad Software, San Diego, CA, USA). Normal distribution was tested using the Kolmogorov-Smirnov test and Shapiro-Wilk test. Normally distributed data of two groups were compared by t-test. For 3 or more groups and repeated measurements, missing data were imputed by mean substitution, and an ANOVA was conducted followed by prespecified constrasts against wild type animals. In case of normal distribution was not given, two groups were compared by a U-test. $*P < 0.05$, $**P < 0.01$, $***P < 0.001$, $****P < 0.0001$. All data are presented as mean ± s.e.m. Hierarchical cluster analysis of the pruritogens was conducted with the mean scratch values of wild type mice using IBM SPSS Statistics (Version 21, IBM, Armonk, NY, US). Distances were calculated using Ward's methods and the squared Euclidean distance.

Data availability

The datasets generated during the current study are available from the corresponding author on reasonable request.

Received: 6 November 2019; Accepted: 17 January 2020;
Published online: 11 February 2020

References

1. Weisshaar, E. *et al.* European guideline on chronic pruritus: In cooperation with the European dermatology forum (EDF) and the European academy of dermatology and venereology (EADV). *Acta Derm. Venereol.* **92**, 563–581 (2012).
2. Simone, D. A. *et al.* The magnitude and duration of itch produced by intracutaneous injections of histamine. *Somatosens. Res.* **5**, 81–92 (1987).
3. Rossbach, K. *et al.* Histamine H1, H3 and H4 receptors are involved in pruritus. *Neuroscience* **190**, 89–102 (2011).
4. Sikand, P., Dong, X. & LaMotte, R. H. BAM8-22 Peptide Produces Itch and Nociceptive Sensations in Humans Independent of Histamine Release. *J. Neurosci.* **31**, 7563–7567 (2011).
5. Liu, Q. *et al.* Sensory Neuron-Specific GPCR Mrgprs Are Itch Receptors Mediating Chloroquine-Induced Pruritus. *Cell* **139**, 1353–1365 (2009).
6. Liu, Q. *et al.* Mechanisms of itch evoked by β-alanine. *J. Neurosci.* **32**, 14532–7 (2012).
7. Liu, Q. *et al.* The distinct roles of two GPCRs, MrgprC11 and PAR2, in itch and hyperalgesia. *Sci. Signal.* **4**, ra45 (2011).
8. Yamaguchi, T., Nagasawa, T., Satoh, M. & Kuraishi, Y. Itch-associated response induced by intradermal serotonin through 5-HT2 receptors in mice. *Neurosci. Res.* **35**, 77–83 (1999).
9. Kremer, A. E. *et al.* Lysophosphatidic acid is a potential mediator of cholestatic pruritus. *Gastroenterology* **139**, 1018.e1–1018 (2010).
10. Chen, Y. *et al.* Luciferase reporter gene assay on human 5-HT receptor: which response element should be chosen? *Sci. Rep.* **5**, 8060 (2015).
11. Han, S.-K. *et al.* Orphan G protein-coupled receptors MrgA1 and MrgC11 are distinctively activated by RF-amide-related peptides through the G q/11 pathway. *Proc. Natl. Acad. Sci.* **99**, 14740–14745 (2002).
12. Shinohara, T. *et al.* Identification of a G protein-coupled receptor specifically responsive to beta-alanine. *J. Biol. Chem.* **279**, 23559–64 (2004).
13. Lembo, P. M. C. *et al.* Proenkephalin A gene products activate a new family of sensory neuron–specific GPCRs. *Nat. Neurosci.* **5**, 201–9 (2002).
14. Sun, S. & Dong, X. Trp channels and itch. *Semin. Immunopathol.* **38**, 293–307 (2016).
15. Eijkelkamp, N. *et al.* Neurological perspectives on voltage-gated sodium channels. *Brain* **135**, 2585–612 (2012).

16. Lai, J., Porreca, F., Hunter, J. C. & Gold, M. S. Voltage-gated sodium channels and hyperalgesia. *Annu. Rev. Pharmacol. Toxicol.* **44**, 371–97 (2004).
17. Harriott, A. M. & Gold, M. S. Contribution of primary afferent channels to neuropathic pain. *Curr. Pain Headache Rep.* **13**, 197–207 (2009).
18. Jurcakova, D. *et al*. Voltage-Gated Sodium Channels Regulating Action Potential Generation in Itch-, Nociceptive-, and Low-Threshold Mechanosensitive Cutaneous C-Fibers. *Mol. Pharmacol.* **94**, 1047–1056 (2018).
19. Usoskin, D. *et al*. Unbiased classification of sensory neuron types by large-scale single-cell RNA sequencing. *Nat. Publ. Gr.* **18**, 145–153 (2014).
20. Zimmermann, K. *et al*. Sensory neuron sodium channel Nav1.8 is essential for pain at low temperatures. *Nature* **447**, 855–8 (2007).
21. Nassar, M. A. *et al*. Nociceptor-specific gene deletion reveals a major role for Nav1.7 (PN1) in acute and inflammatory pain. *Proc. Natl. Acad. Sci.* **101**, 12706–12711 (2004).
22. Dib-Hajj, S. D. *et al*. Voltage-gated sodium channels in pain states: Role in pathophysiology and targets for treatment. *Brain Res. Rev.* **60**, 65–83 (2009).
23. Emery, E. C., Luiz, A. P. & Wood, J. N. Nav 1. 7 and other voltage-gated sodium channels as drug targets for pain relief. *Expert Opin. Ther. Targets* **20**, 975–983 (2016).
24. Zakrzewska, J. M. *et al*. Novel design for a phase IIa placebo-controlled, double-blind randomized withdrawal study to evaluate the safety and efficacy of CNV1014802 in patients with trigeminal neuralgia. *Trials* **14**, 402 (2013).
25. McDonnell, A. *et al*. Efficacy of the Nav1.7 blocker PF-05089771 in a randomised, placebo-controlled, double-blind clinical study in subjects with painful diabetic peripheral neuropathy. *Pain* **159**, 1465–1476 (2018).
26. Devigili, G. *et al*. Paroxysmal itch caused by gain-of-function Nav1.7 mutation. *Pain* **155**, 1702–1707 (2014).
27. Faber, C. G. *et al*. Gain-of-function Nav1.8 mutations in painful neuropathy. *Proc. Natl. Acad. Sci. USA* **109**, 19444–9 (2012).
28. Salvatierra, J. *et al*. A disease mutation reveals a role for NaV1.9 in acute itch. *J. Clin. Invest.* **128**, 5434–5447 (2018).
29. Woods, C. G., Babiker, M. O. E., Horrocks, I., Tolmie, J. & Kurth, I. The phenotype of congenital insensitivity to pain due to the NaV1.9 variant p.L811P. *Eur. J. Hum. Genet.* **23**, 1434 (2015).
30. Lee, J. H. *et al*. A monoclonal antibody that targets a NaV1.7 channel voltage sensor for pain and itch relief. *Cell* **157**, 1393–1404 (2014).
31. Graceffa, R. F. *et al*. Sulfonamides as Selective NaV1.7 Inhibitors: Optimizing Potency, Pharmacokinetics, and Metabolic Properties to Obtain Atropisomeric Quinolinone (AM-0466) that Affords Robust *in Vivo* Activity. *J. Med. Chem.* **60**, 5990–6017 (2017).
32. Kornecook, T. J. *et al*. Pharmacologic Characterization of AMG8379, a Potent and Selective Small Molecule Sulfonamide Antagonist of the Voltage-Gated Sodium Channel Na_V 1.7. *J. Pharmacol. Exp. Ther.* **362**, 146–160 (2017).
33. La, D. S. *et al*. The discovery of benzoxazine sulfonamide inhibitors of NaV1.7: Tools that bridge efficacy and target engagement. *Bioorganic Med. Chem. Lett.* **27**, 3477–3485 (2017).
34. Theile, J. W., Fuller, M. D. & Chapman, M. L. The Selective Nav1.7 Inhibitor, PF-05089771, Interacts Equivalently with Fast and Slow Inactivated Nav1.7 Channels. *Mol. Pharmacol.* **90**, 540–548 (2016).
35. Swain, N. A. *et al*. Discovery of Clinical Candidate 4-[2-(5-Amino-1H-pyrazol-4-yl)-4-chlorophenoxy]-5-chloro-2-fluoro-N-1,3-thiazol-4-ylbenzenesulfonamide (PF-05089771): Design and Optimization of Diaryl Ether Aryl Sulfonamides as Selective Inhibitors of NaV1.7. *J. Med. Chem.* **60**, 7029–7042 (2017).
36. Jarvis, M. F. *et al*. A-803467, a potent and selective Nav1.8 sodium channel blocker, attenuates neuropathic and inflammatory pain in the rat. *Proc. Natl. Acad. Sci.* **104**, 8520–8525 (2007).
37. Reich, A., Ständer, S. & Szepietowski, J. C. Drug-induced pruritus: A review. *Acta Derm. Venereol.* **89**, 236–244 (2009).
38. Shields, S. D. *et al*. Insensitivity to Pain upon Adult-Onset Deletion of Nav1.7 or Its Blockade with Selective Inhibitors. *J. Neurosci.* **38**, 10180–10201 (2018).
39. Klugbauer, N., Lacinova, L., Flockerzi, V. & Hofmann, F. Structure and functional expression of a new member of the tetrodotoxin-sensitive voltage-activated sodium channel family from human neuroendocrine cells. *EMBO J.* **14**, 1084–90 (1995).
40. Cummins, T. R., Sheets, P. L. & Waxman, S. G. The roles of sodium channels in nociception: Implications for mechanisms of pain. *Pain* **131**, 243–57 (2007).
41. Choi, J.-S., Dib-Hajj, S. D. & Waxman, S. G. Inherited erythermalgia: limb pain from an S4 charge-neutral Na channelopathy. *Neurology* **67**, 1563–7 (2006).
42. Cummins, T. R., Dib-Hajj, S. D. & Waxman, S. G. Electrophysiological properties of mutant Nav1.7 sodium channels in a painful inherited neuropathy. *J. Neurosci.* **24**, 8232–6 (2004).
43. Sheets, P. L., Jackson, J. O., Waxman, S. G., Dib-Hajj, S. D. & Cummins, T. R. A Nav1.7 channel mutation associated with hereditary erythromelalgia contributes to neuronal hyperexcitability and displays reduced lidocaine sensitivity. *J. Physiol.* **581**, 1019–31 (2007).
44. McDermott, L. A. *et al*. Defining the Functional Role of NaV1.7 in Human Nociception. *Neuron* **101**, 905–919.e8 (2019).
45. Gingras, J. *et al*. Global Nav1.7 knockout mice recapitulate the phenotype of human congenital indifference to pain. *PLoS One* **9**, (2014).
46. Han, C., Huang, J. & Waxman, S. G. Sodium channel Nav1.8: Emerging links to human disease. *Neurology* **86**, 473–83 (2016).
47. Sangameswaran, L. *et al*. Structure and function of a novel voltage-gated, tetrodotoxin-resistant sodium channel specific to sensory neurons. *J. Biol. Chem.* **271**, 5953–6 (1996).
48. Elliott, A. A. & Elliott, J. R. Characterization of TTX-sensitive and TTX-resistant sodium currents in small cells from adult rat dorsal root ganglia. *J. Physiol.* **463**, 39–56 (1993).
49. Hoffmann, T. *et al*. Reduced excitability and impaired nociception in peripheral unmyelinated fibers from Nav1.9-null mice. *Pain* **158**, 58–67 (2017).
50. Nicol, N. H. Anatomy and physiology of the skin. *Dermatology Nurs.* **17**, 62 (2005).
51. Akopian, A. N. *et al*. The tetrodotoxin-resistant sodium channel SNS has a specialized function in pain pathways. *Nat. Neurosci.* **2**, 541–8 (1999).
52. Matsutomi, T., Nakamoto, C., Zheng, T., Kakimura, J.-I. & Ogata, N. Multiple types of Na(+) currents mediate action potential electrogenesis in small neurons of mouse dorsal root ganglia. *Pflugers Arch.* **453**, 83–96 (2006).
53. Weiss, J. *et al*. Loss-of-function mutations in sodium channel Nav1.7 cause anosmia. *Nature* **472**, 186–90 (2011).
54. Ostman, J. A. R., Nassar, M. A., Wood, J. N. & Baker, M. D. GTP up-regulated persistent Na+ current and enhanced nociceptor excitability require NaV1.9. *J. Physiol.* **586**, 1077–87 (2008).
55. Cummins, T. R., Howe, J. R. & Waxman, S. G. Slow closed-state inactivation: a novel mechanism underlying ramp currents in cells expressing the hNE/PN1 sodium channel. *J. Neurosci.* **18**, 9607–19 (1998).
56. Herzog, R. I., Cummins, T. R., Ghassemi, F., Dib-Hajj, S. D. & Waxman, S. G. Distinct repriming and closed-state inactivation kinetics of Nav1.6 and Nav1.7 sodium channels in mouse spinal sensory neurons. *J. Physiol.* **551**, 741–750 (2003).
57. Isensee, J. *et al*. Synergistic regulation of serotonin and opioid signaling contributes to pain insensitivity in Nav1.7 knockout mice. *Sci. Signal.* **10**, (2017).
58. Liu, X.-Y. *et al*. Unidirectional cross-activation of GRPR by MOR1D uncouples itch and analgesia induced by opioids. *Cell* **147**, 447–58 (2011).
59. Ringkamp, M. *et al*. A role for nociceptive, myelinated nerve fibers in itch sensation. *J. Neurosci.* **31**, 14841–9 (2011).
60. Minett, M. S. *et al*. Distinct Nav1.7-dependent pain sensations require different sets of sensory and sympathetic neurons. *Nat. Commun.* **3**, 791–799 (2012).

61. Faul, F., Erdfelder, E., Lang, A.-G. & Buchner, A. G*Power 3: a flexible statistical power analysis program for the social, behavioral, and biomedical sciences. *Behav. Res. Methods* **39**, 175–91 (2007).
62. Dittert, I. *et al*. A technique for fast application of heated solutions of different composition to cultured neurones. *J. Neurosci. Methods* **82**, 195–201 (1998).
63. Livak, K. J. & Schmittgen, T. D. Analysis of relative gene expression data using real-time quantitative PCR and the 2(-Delta Delta C(T)) Method. *Methods* **25**, 402–8 (2001).

Acknowledgements

This work was supported by the German Research Foundation to AEK (KR4391/1-1; KR3618/3-1). Additional funding was provided by the interdisciplinary center for clinical research (IZKF) at the Friedrich-Alexander-University of Erlangen-Nürnberg within grant E20 to AEK and within grant E27 to AEK and MF. Annette Kuhn and Iwona Izydorczyk provided excellent technical support. The authors have no financial or other relationships to report that might lead to conflict of interest.

Author contributions

H.K., M.J.M.F. and A.E.K. designed the study; H.K., L.K. and L.G. acquired data; H.K., L.K., K.W., L.G., M.F.N., P.R., M.J.M.F., A.E.K. analysed and interpreted the data; H.K. drafted the manuscript with the help of A.E.K. and M.J.M.F.; L.K., K.W., L.G., M.F.N., P.R., M.J.M.F., A.E.K. critically revised the manuscript.

Competing interests

The authors declare no competing interests.

Additional information

Supplementary information is available for this paper at https://doi.org/10.1038/s41598-020-59092-2.

Correspondence and requests for materials should be addressed to H.K. or A.E.K.

Reprints and permissions information is available at www.nature.com/reprints.

Publisher's note Springer Nature remains neutral with regard to jurisdictional claims in published maps and institutional affiliations.